Supporting Information

Structural design strategies for superionic sodium halide solid electrolytes

Seungho Yu,[a,b,*], Kwangnam Kim,[c] Brandon C. Wood,[c] Hun-Gi Jung, [a,b] Kyung Yoon Chung, [a,b]

[a]Energy Storage Research Center, Korea Institute of Science and Technology, 5, Hwarang-ro 14-gil, Seongbuk-gu, Seoul 02792, Republic of Korea

[b]Division of Energy & Environment Technology, KIST School, Korea University of Science and Technology, Seoul 02792, Republic of Korea

[c]Materials Science Division, Lawrence Livermore National Laboratory, Livermore, 94550, USA

Corresponding Author

[*]E-mail: shyu@kist.re.kr

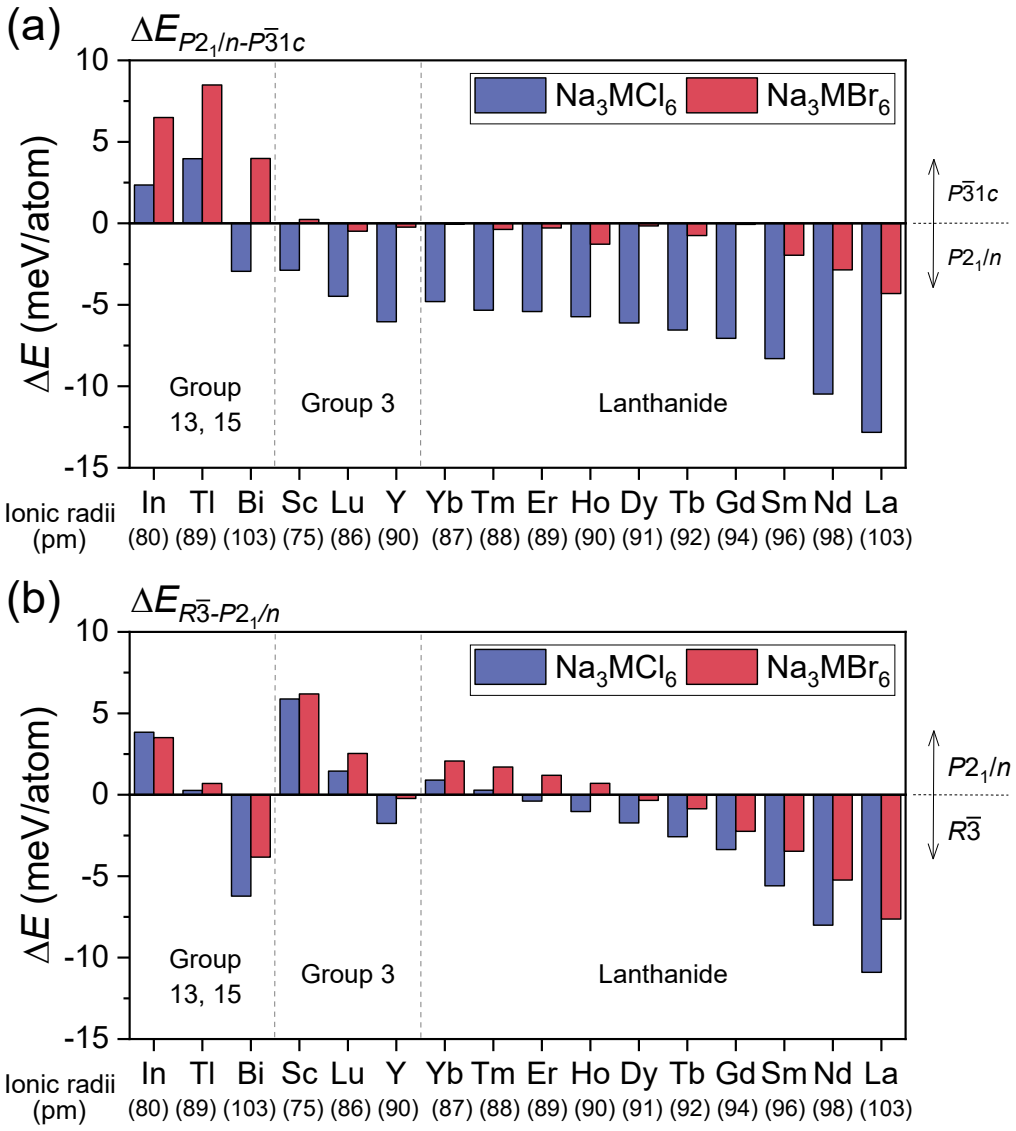

Figure S1. Energy differences among the crystal structures of (a) $P\bar{3}1c$ and $P2_1/n$, (b) $R\bar{3}$ and $P2_1/n$ for Na_3MX_6 (X = Cl and Br), as a function of the effective ionic radii of M in group 13 and 15 elements, group 3 elements and lanthanides.

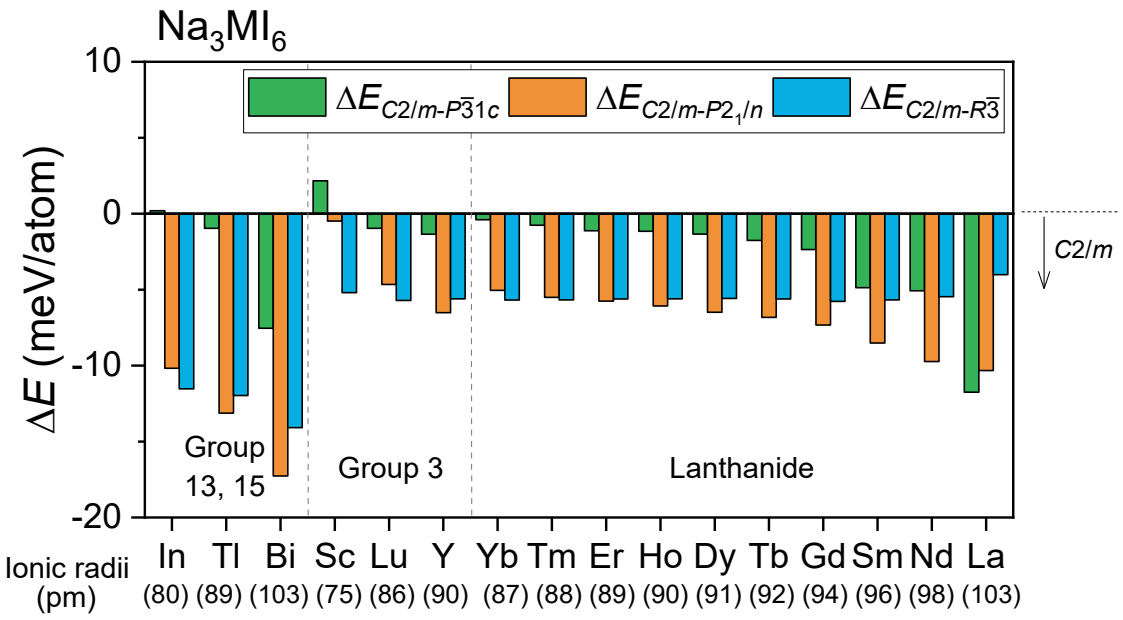

Figure S2. Energy differences of the crystal structures of $P\bar{3}1c$, $P2_1/n$ and $R\bar{3}$ against the crystal structure of $C2/m$ for Na_3MI_6 ($\Delta E_{C2/m-P31c}$ (orange), $\Delta E_{C2/m-P21/n}$ (green) and $\Delta E_{C2/m-R3}$ (light blue)), as a function of the effective ionic radii of M in group 13 and 15 elements, group 3 elements and lanthanides. Negative values of ΔE indicate the preference of the $C2/m$ phase compared to other phases.

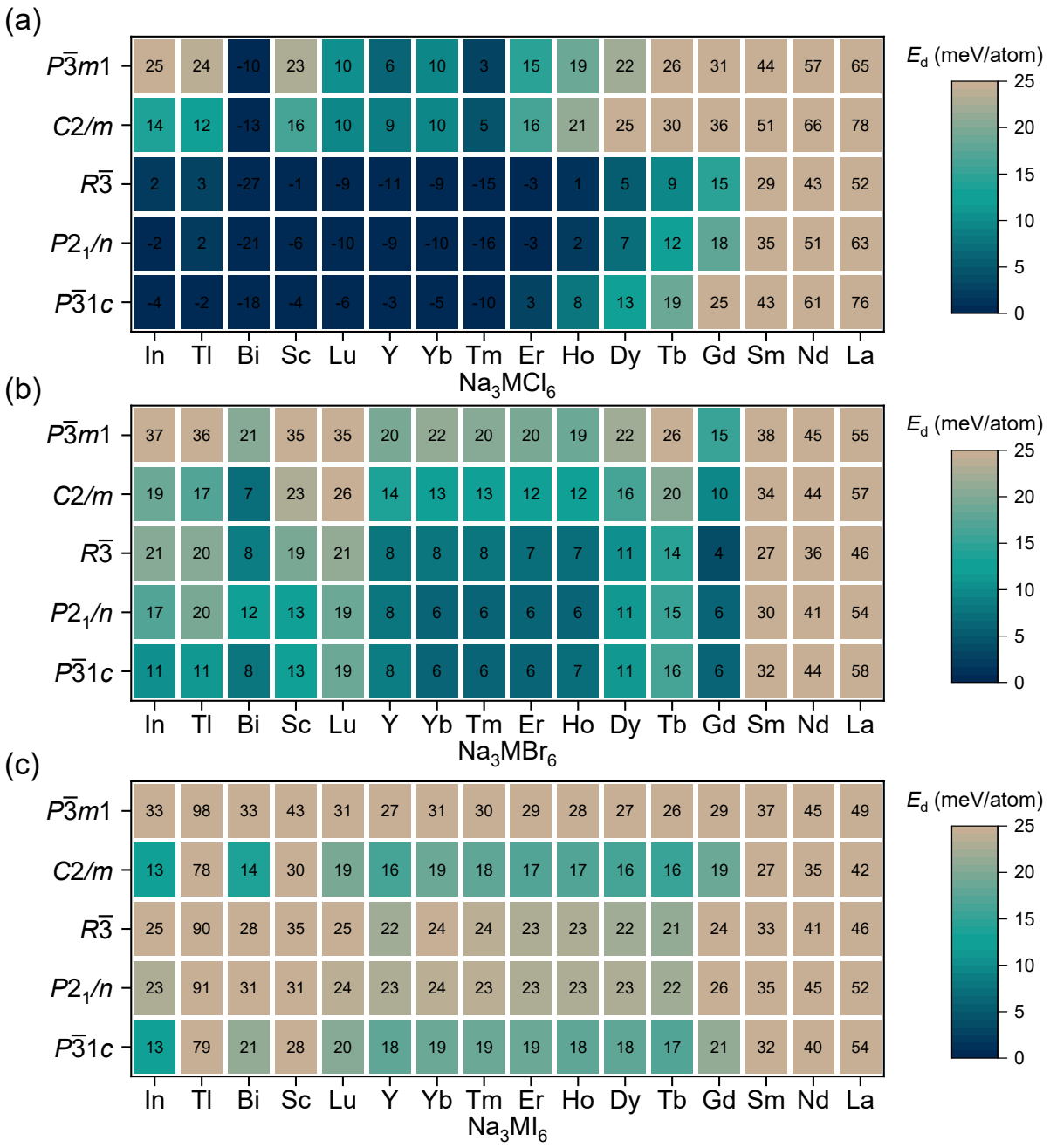

Figure S3. Heat map of the decomposition energy (E_d) for sodium halides (a) Na_3MCl_6, (b) Na_3MBr_6 and (c) Na_3MI_6 with the crystal structures of $P\bar{3}1c$, $P2_1/n$, $R\bar{3}$, $C2/m$ and $P\bar{3}m1$. The values of E_d for Na_3MX_6 (X = Cl, Br, I) are shown in the heat map.

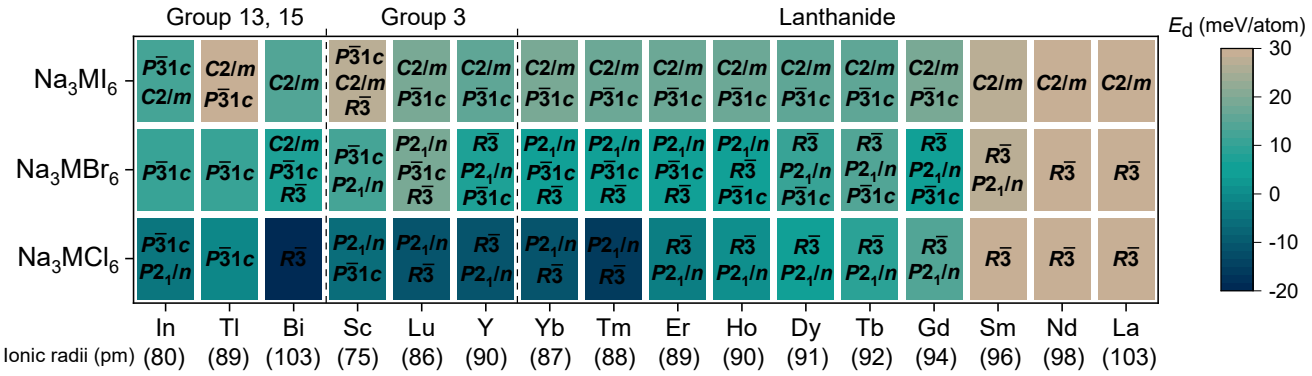

Figure S4. Heat map for the decomposition energy (E_d) of Na halides (Na_3MX_6, X = Cl, Br, and I) against the competing phases NaX and MX_3. The most stable phase among the crystal structures of $P\bar{3}1c$, $P2_1/n$, $R\bar{3}$, $C2/m$ and $P\bar{3}m1$ was used to evaluate E_d. The most stable and were indicated in Figure 1(a), while the other phases were also denoted in Figure S4 when the decomposition energy (E_d) was comparable within 3 meV/atom.

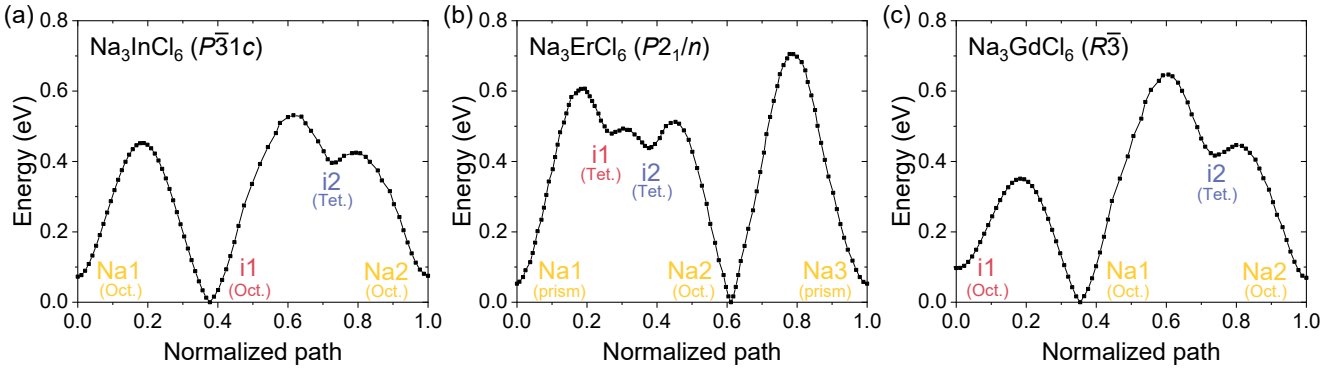

Figure S5. Na-ion migration energy barriers along the migration paths in (a) Na_3InCl_6 (trigonal $P\bar{3}1c$), (b) Na_3ErCl_6 (monoclinic $P2_1/n$) and (c) Na_3GdCl_6 (trigonal $R\bar{3}$) calculated using the BVSE method.

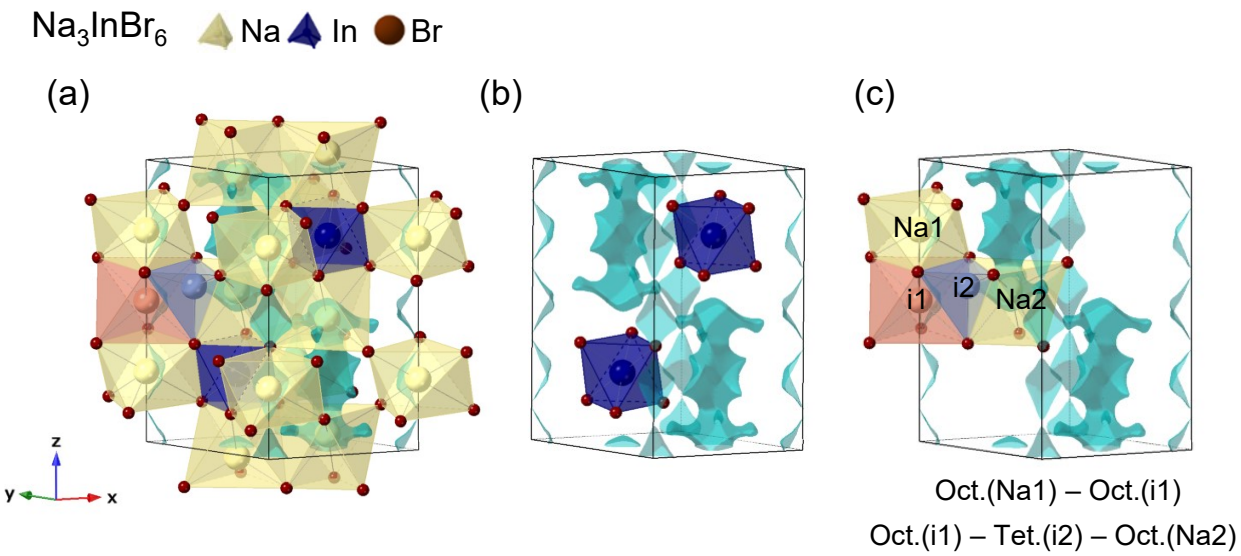

Figure S6. Na-ion potential energy landscape of Na_3InBr_6 (trigonal $P\bar{3}1c$) calculated using the BVSE method, including (a-b) the isosurface of Na-ion probability distribution (light blue), $NaBr_6$ and $InBr_6$ octahedra (yellow and blue, respectively), (c) one-dimensional path between octahedral sites (Na1-i1) and three-dimensional path between octahedral sites via tetrahedral interstitial sites (i1-i2-Na2).

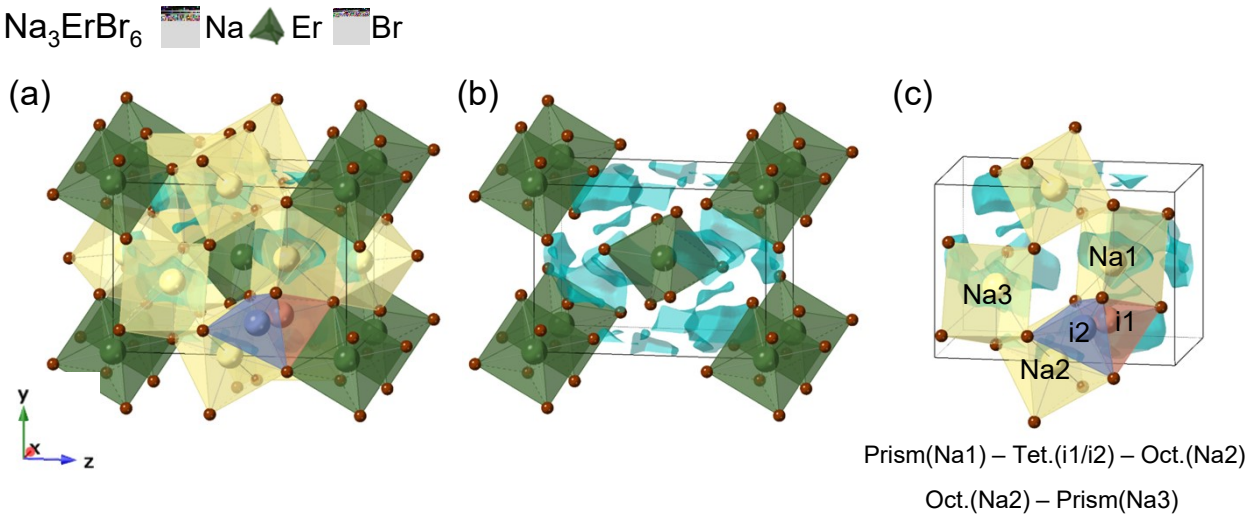

Figure S7. Na-ion potential energy landscape of Na_3ErBr_6 (monoclinic $P2_1/n$) calculated using the BVSE method, including (a-b) the isosurface of Na-ion probability distribution (light blue), $NaBr_6$ and $ErBr_6$ octahedra (yellow and dark green, respectively), (c) migration paths between octahedral and prism sites via tetrahedral interstitial sites (Na1-i1/i2-Na2) and between octahedral and prism sites (Na2-Na3).

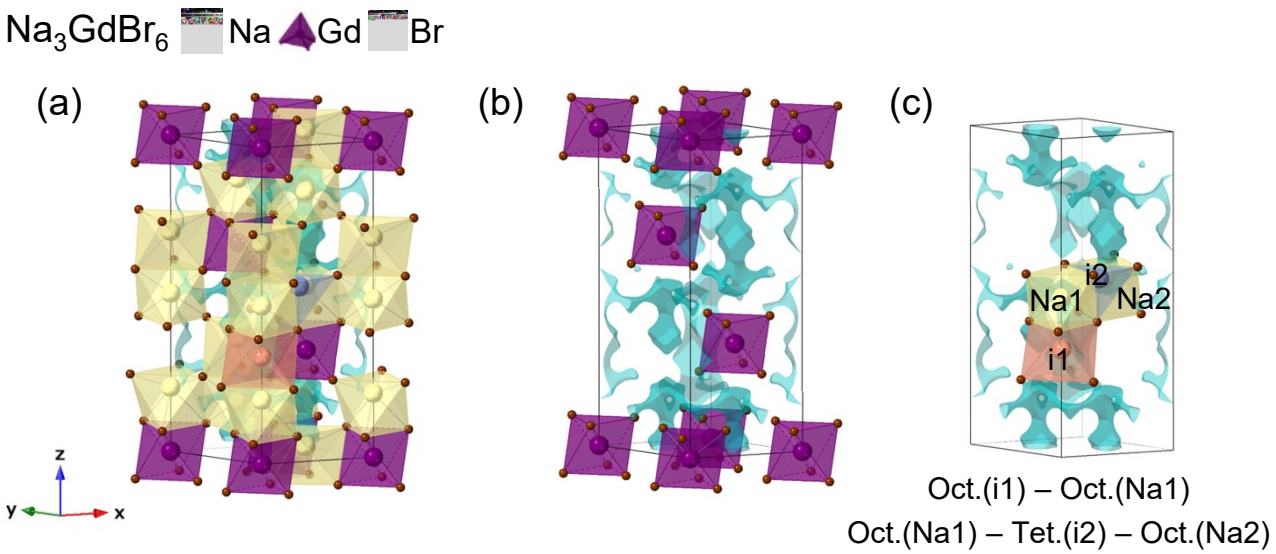

Figure S8. Na-ion potential energy landscape of Na_3GdBr_6 (trigonal $R\bar{3}$) calculated using the BVSE method, including (a-b) the isosurface of Na-ion probability distribution (light blue), $NaBr_6$ and $GdBr_6$ octahedra (yellow and purple, respectively), (c) one-dimensional path between octahedral sites (i1-Na1) and three-dimensional path between octahedral sites via tetrahedral interstitial sites (Na1-i2-Na2).

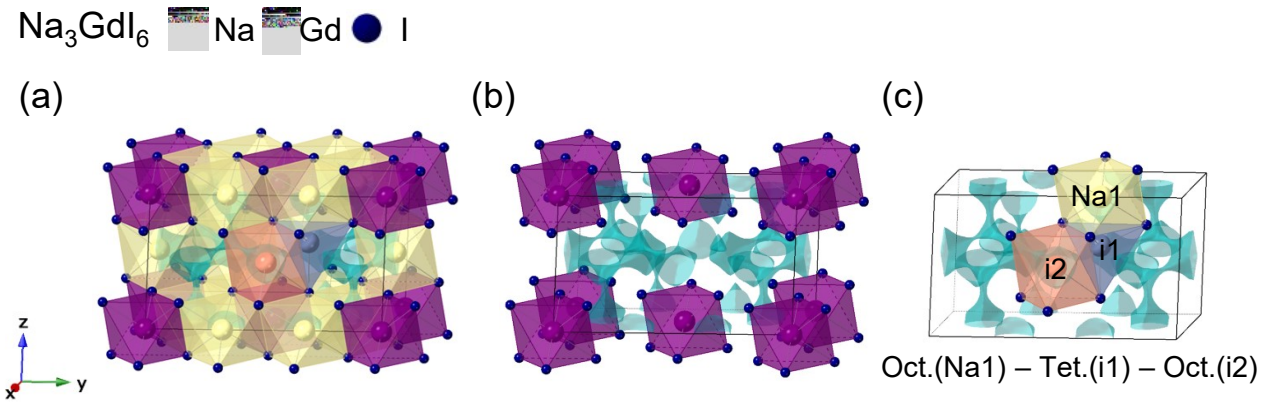

Figure S9. Na-ion potential energy landscape of Na_3GdI_6 (monoclinic *C*2/*m*) calculated using the BVSE method, including (a-b) the isosurface of Na-ion probability distribution (light blue), NaI_6 and GdI_6 octahedra (yellow and purple, respectively), (c) three-dimensional path between octahedral sites via tetrahedral interstitial sites (Na1-i1-i2).

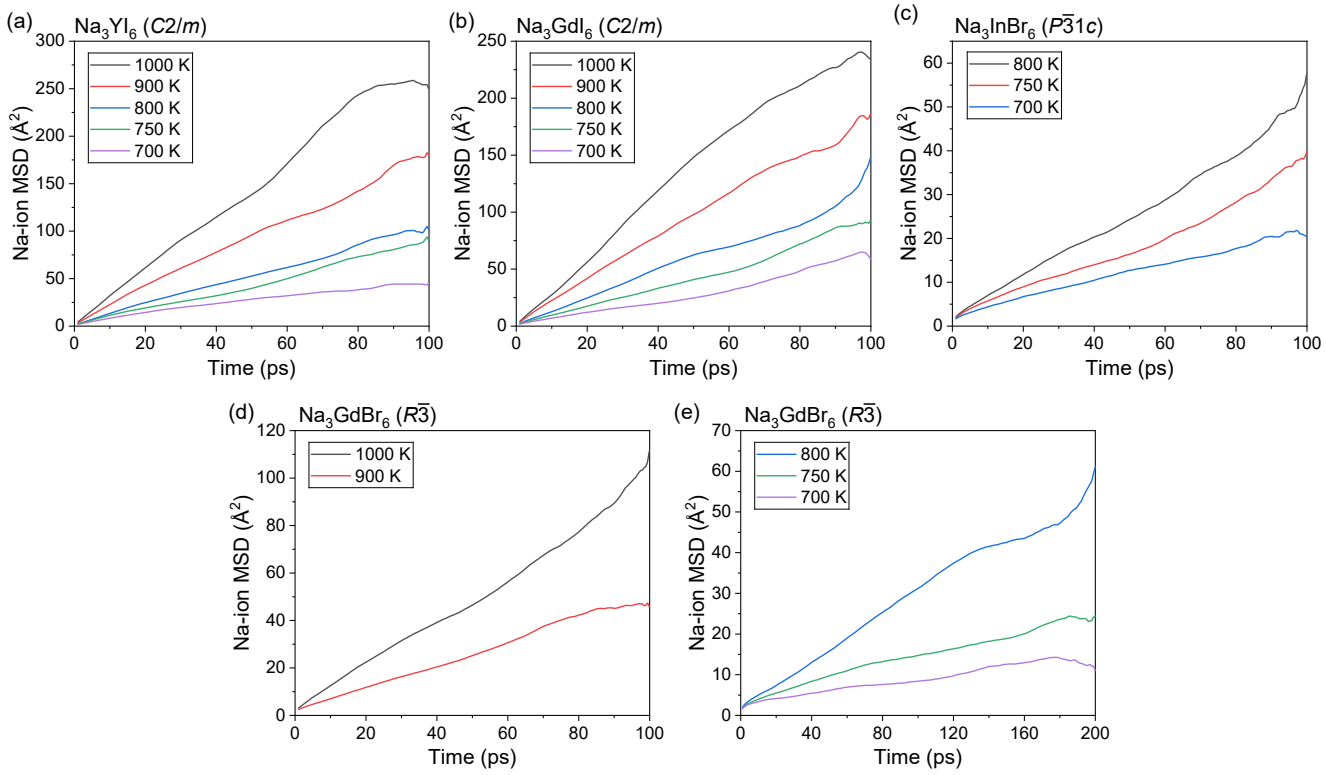

Figure S10. Na-ion MSD at 700–1000 K for (a) Na_3YI_6 (monoclinic $C2/m$), (b) Na_3GdI_6 (monoclinic $C2/m$), (c) Na_3InBr_6 (trigonal $P\bar{3}1c$), (d, e) Na_3GdBr_6 (trigonal $R\bar{3}$).

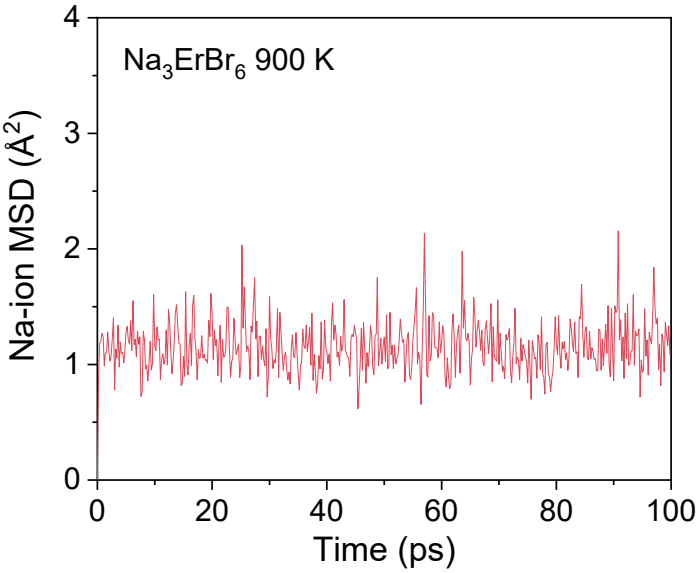

Figure S11. Na-ion MSD over a 100-ps window for $Na_3ErBrCl_6$ at 900 K.

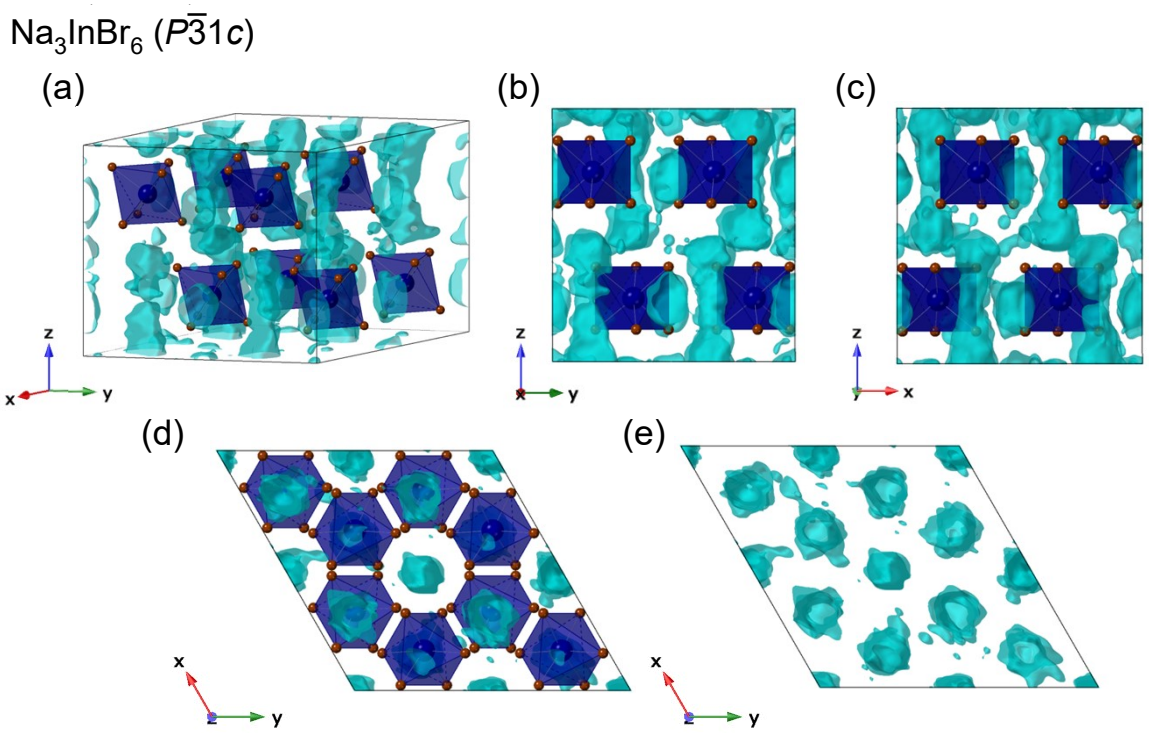

Figure S12. Isosurfaces of the Na-ion probability densities (light blue) from 50 ps AIMD calculations at 800 K plotted using an isosurface value of $2P_0$ for Na_3InBr_6 (trigonal $P\bar{3}1c$), with the view along x, y, z directions. The blue octahedra corresponds to $InBr_6$.

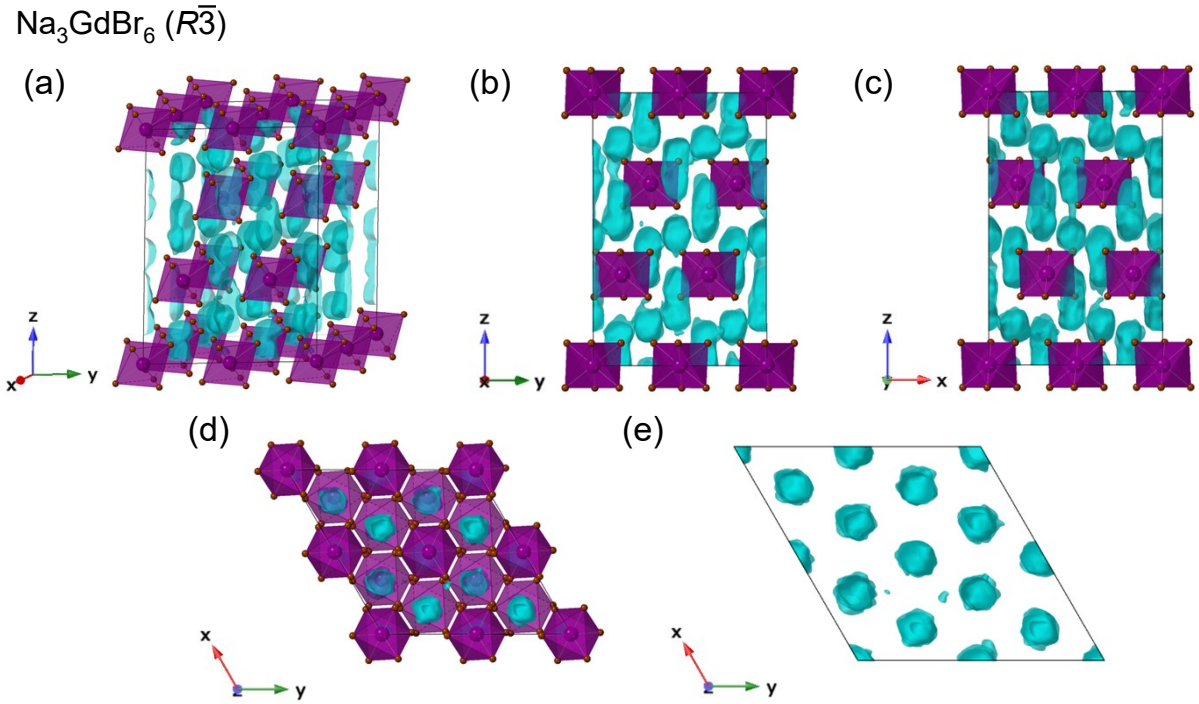

Figure S13. Isosurfaces of the Na-ion probability densities (light blue) from 50 ps AIMD calculations at 800 K plotted using an isosurface value of $2P_0$ for Na_3GdBr_6 (trigonal $R\bar{3}$), with the view along x, y, z directions. The purple octahedra corresponds to $GdBr_6$.

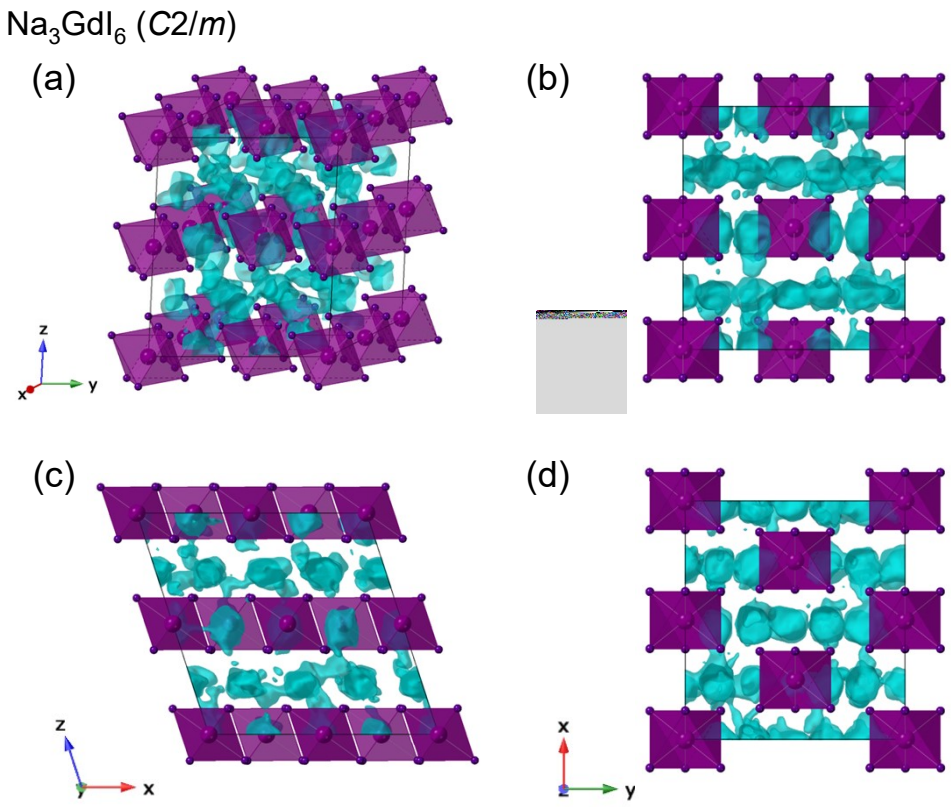

Figure S14. Isosurfaces of the Na-ion probability densities (light blue) from 50 ps AIMD calculations at 800 K plotted using an isosurface value of $2P_0$ for Na_3GdI_6 (monoclinic $C2/m$), with the view along x, y, z directions. The purple octahedra corresponds to GdI_6.

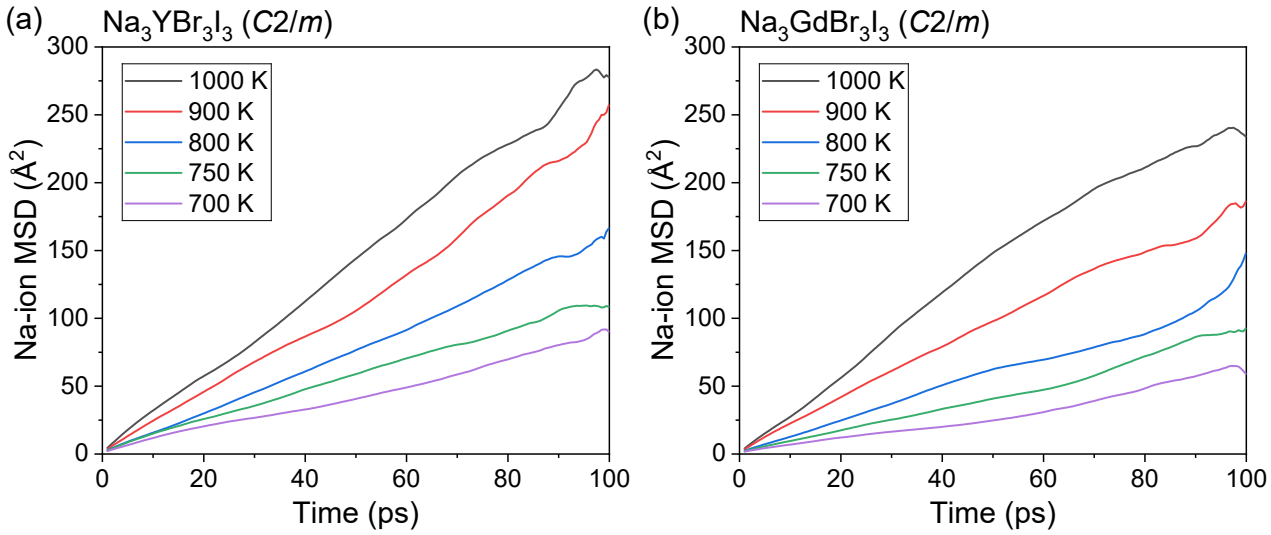

Figure S15. Na-ion MSD at 700–1000 K for monoclinic *C*2/*m* (a) $Na_3YBr_3I_3$ and (b) $Na_3GdBr_3I_3$.

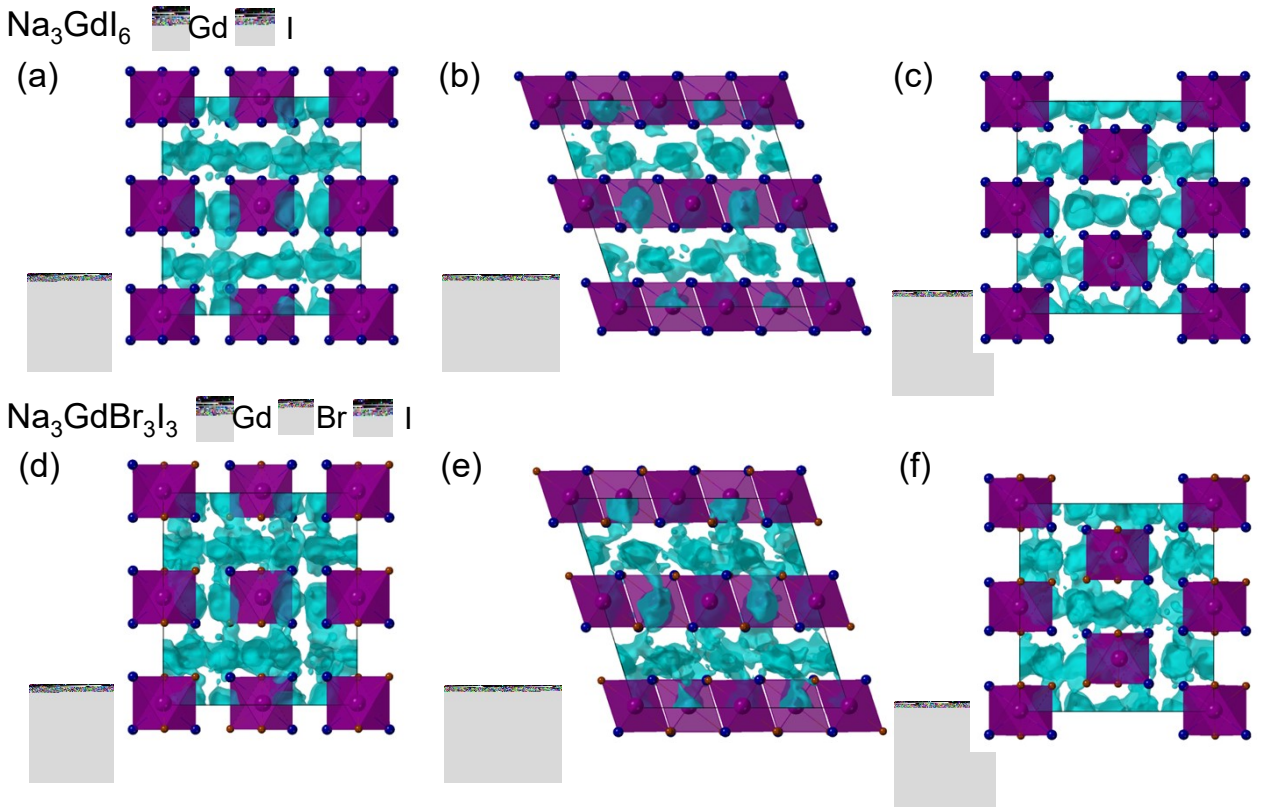

Figure S16. Isosurfaces of the Na-ion probability densities (light blue) from 50 ps AIMD calculations at 800 K plotted using an isosurface value of $2P_0$ for (a-c) Na_3GdI_6 and (d-f) $Na_3GdBr_3I_3$, with the view along x, y, z directions.

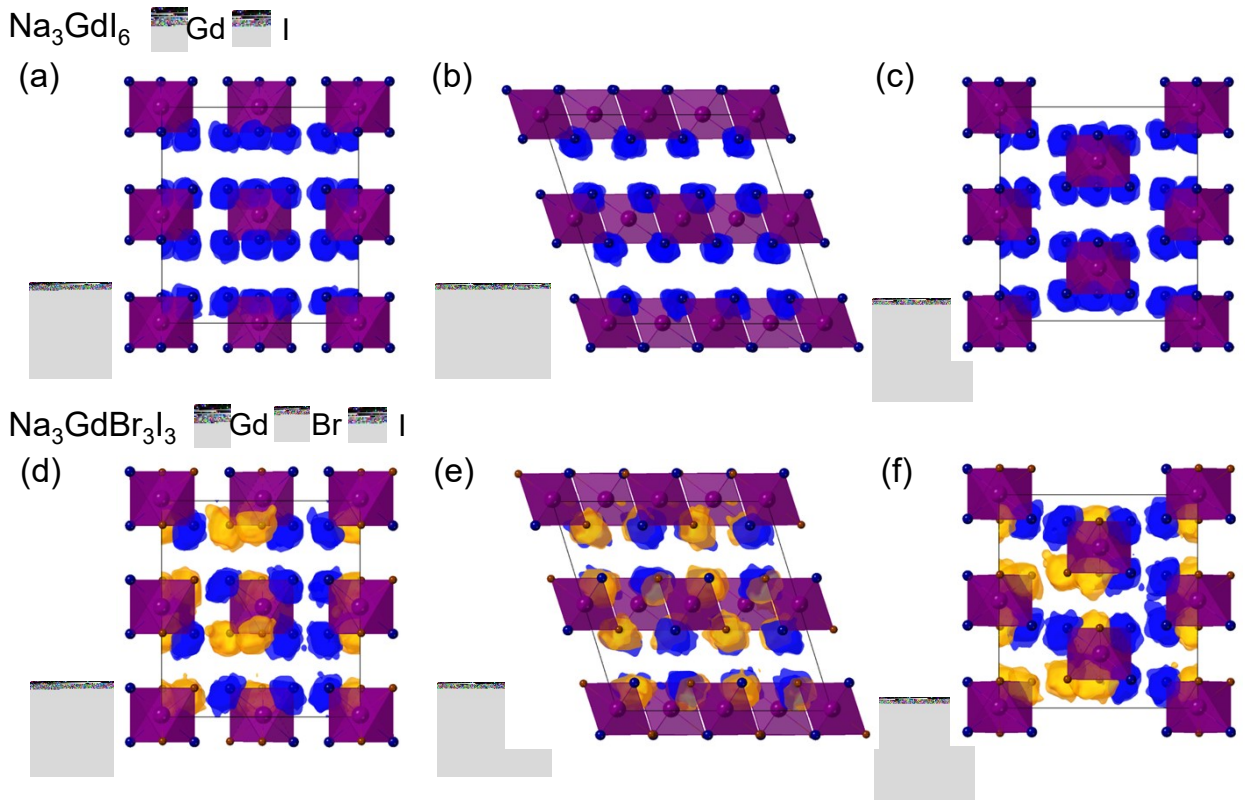

Figure S17. Isosurfaces of the ionic probability densities for Br and I (blue and orange, respectively) from 50 ps AIMD calculations at 800 K plotted using an isosurface value of $2P_0$ for (a-c) Na_3GdI_6 and (d-f) $Na_3GdBr_3I_3$, with the view along x, y, z directions.

Table S1. Details of the structural information of fully occupied *C2/m* and $P\bar{3}m1$ phases.

Space group	monoclinic *C2/m*			trigonal $P\bar{3}m1$			
Space group number	12			164			
Compound	Li_3ScCl_6			Li_3YCl_6			
Lattice a (Å)	6.2593			11.0426			
Lattice b (Å)	10.9587			11.0426			
Lattice c (Å)	6.2465			6.0124			
Angle α (°)	90			90			
Angle β (°)	108.588			90			
Angle γ (°)	90			120			
Ionic Position	Li1	0.5000	0.3285	0.5000	Li1	0.3397	0.3397	0.0000
	Li2	0.5000	0.0000	0.5000	Li2	0.6603	0.0000	0.0000
	Li3	0.5000	0.8264	0.0000	Li3	0.0000	0.6603	0.0000
	Li4	0.5000	0.1736	0.0000	Li4	0.6603	0.6603	0.0000
	Li5	0.0000	0.3264	0.0000	Li5	0.3397	0.0000	0.0000
	Li6	0.0000	0.6736	0.0000	Li6	0.0000	0.3397	0.0000
	Sc1	0.0000	0.0000	0.0000	Li7	0.6700	0.0000	0.5000
	Sc2	0.5000	0.5000	0.0000	Li8	0.0000	0.6700	0.5000
	Cl1	0.2393	0.8391	0.2365	Li9	0.3300	0.3300	0.5000
	Cl2	0.7607	0.8391	0.7635	Y1	0.0000	0.0000	0.0000
	Cl3	0.7607	0.1609	0.7635	Y2	0.3333	0.6667	0.5100
	Cl4	0.2393	0.1609	0.2365	Y3	0.6667	0.3333	0.4900
	Cl5	0.7393	0.3391	0.2365	Cl1	0.1135	0.8865	0.7681
	Cl6	0.2607	0.3391	0.7635	Cl2	0.1135	0.2270	0.7681
	Cl7	0.2607	0.6609	0.7635	Cl3	0.7730	0.8865	0.7681
	Cl8	0.7393	0.6609	0.2365	Cl4	0.8865	0.1135	0.2319
	Cl9	0.7590	0.0000	0.2324	Cl5	0.2270	0.1135	0.2319
	Cl10	0.2410	0.0000	0.7676	Cl6	0.8865	0.7730	0.2319
	Cl11	0.2590	0.5000	0.2324	Cl7	0.2215	0.7785	0.2676
	Cl12	0.7410	0.5000	0.7676	Cl8	0.2215	0.4430	0.2676
					Cl9	0.5570	0.7785	0.2676
					Cl10	0.7785	0.2215	0.7324
					Cl11	0.4430	0.2215	0.7324
					Cl12	0.7785	0.5570	0.7324
					Cl13	0.4454	0.5546	0.7559
					Cl14	0.4454	0.8908	0.7559
					Cl15	0.1092	0.5546	0.7559
					Cl16	0.5546	0.4454	0.2441
					Cl17	0.8908	0.4454	0.2441
					Cl18	0.5546	0.1092	0.2441

Table S2. Total energy differences among the crystal structures of $P\bar{3}1c$, $P2_1/n$, $R\bar{3}$, $C2/m$ and $P\bar{3}m1$ for Na_3MX_6 (X = Cl, Br, I).

Na_3MX_6	Type of M	ΔE (meV/atom)				
		$P2_1/n$ - $P\bar{3}1c$	$R\bar{3}$ - $P2_1/n$	$R\bar{3}$ - $P\bar{3}1c$	$C2/m$ - $P2_1/n$	$C2/m$ - $R\bar{3}$
Na_3AlCl_6	Group 13	-0.1	12.1	12.0	28.0	16.0
Na_3GaCl_6		2.5	10.7	13.2	21.9	11.1
Na_3InCl_6		2.4	3.8	6.2	16.0	12.1
Na_3TlCl_6		4.0	0.3	4.2	9.7	9.4
Na_3BiCl_6	Group 15	-2.9	-6.2	-9.2	8.0	14.2
Na_3ScCl_6	Group 3	-2.9	5.9	3.0	22.4	16.6
Na_3LuCl_6		-4.5	1.5	-3.0	20.2	18.8
Na_3YCl_6		-6.0	-1.8	-7.8	18.4	20.1
Na_3YbCl_6	Lanthanide	-4.8	0.9	-3.9	19.9	19.0
Na_3TmCl_6		-5.3	0.3	-5.1	20.2	19.9
Na_3ErCl_6		-5.4	-0.4	-5.8	19.1	19.5
Na_3HoCl_6		-5.7	-1.0	-6.8	18.7	19.7
Na_3DyCl_6		-6.1	-1.7	-7.8	18.3	20.0
Na_3TbCl_6		-6.6	-2.6	-9.1	17.9	20.5
Na_3GdCl_6		-7.1	-3.4	-10.4	17.5	20.9
Na_3SmCl_6		-8.3	-5.6	-13.9	16.4	21.9
Na_3NdCl_6		-10.5	-8.0	-18.5	15.5	23.5
Na_3LaCl_6		-12.8	-10.9	-23.7	14.7	25.6
Na_3AlBr_6	Group 13	3.2	10.8	14.1	12.2	1.4
Na_3GaBr_6		5.8	9.2	15.0	6.8	-2.4
Na_3InBr_6		6.5	3.5	10.0	1.5	-2.1
Na_3TlBr_6		8.5	0.7	9.2	-2.6	-3.3
Na_3BiBr_6	Group 15	4.0	-3.8	0.1	-5.2	-1.4
Na_3ScBr_6	Group 3	0.2	6.2	6.4	9.8	3.7
Na_3LuBr_6		-0.5	2.5	2.0	7.4	4.9
Na_3YBr_6		-0.2	-0.2	-0.5	5.4	5.7
Na_3YbBr_6	Lanthanide	-0.1	2.1	2.0	6.9	4.8
Na_3TmBr_6		-0.4	1.7	1.3	6.6	4.9
Na_3ErBr_6		-0.3	1.2	0.9	6.4	5.2

Na_3HoBr_6		-1.3	0.7	-0.6	6.0	5.3
Na_3DyBr_6		-0.2	-0.3	-0.5	5.1	5.4
Na_3TbBr_6		-0.8	-0.9	-1.6	4.7	5.6
Na_3GdBr_6		-0.1	-2.2	-2.3	3.7	6.0
Na_3SmBr_6		-2.0	-3.5	-5.4	3.2	6.7
Na_3NdBr_6		-2.9	-5.2	-8.1	2.7	7.9
Na_3LaBr_6		-4.3	-7.6	-11.9	2.5	10.1
Na_3AlI_6	Group 13	5.1	6.7	11.8	-0.9	-7.6
Na_3GaI_6		7.0	6.2	13.1	-3.6	-9.7
Na_3InI_6		10.4	1.3	11.7	-10.2	-11.5
Na_3TlI_6		12.2	-1.2	11.0	-13.1	-12.0
Na_3BiI_6	Group 15	9.7	-3.2	6.5	-17.3	-14.1
Na_3ScI_6	Group 3	2.7	4.7	7.4	-0.5	-5.2
Na_3LuI_6		3.7	1.0	4.7	-4.7	-5.7
Na_3YI_6		5.2	-0.9	4.2	-6.5	-5.6
Na_3YbI_6	Lanthanide	4.6	0.6	5.3	-5.0	-5.7
Na_3TmI_6		4.7	0.2	4.9	-5.5	-5.7
Na_3ErI_6		4.6	-0.1	4.5	-5.8	-5.6
Na_3HoI_6		4.9	-0.5	4.4	-6.1	-5.6
Na_3DyI_6		5.1	-0.9	4.2	-6.5	-5.6
Na_3TbI_6		5.1	-1.2	3.8	-6.8	-5.6
Na_3GdI_6		5.0	-1.6	3.4	-7.3	-5.8
Na_3SmI_6		3.6	-2.8	0.8	-8.5	-5.7
Na_3NdI_6		4.7	-4.3	0.4	-9.7	-5.5
Na_3LaI_6		-1.4	-6.3	-7.7	-10.3	-4.0

Table S3. Crystal structure of MX_3 (X = Cl, Br, I) in the Inorganic Crystal Structure Database (ICSD). If MX_3 phase is not available in the ICSD, most stable phase among the experimental structures was predicted.

MX_3	Type of M	M_{Radii} (pm)	ICSD ID	Space group	Crystal system	Predicted phase
$AlCl_3$	Group 13	53.5	39566	*C*2/*m* (12)	Monoclinic	
$GaCl_3$		62	413455	*C*2/*m* (12)	Monoclinic	
$InCl_3$		80	N/A			$R\bar{3}$ (148)
$TlCl_3$		88.5	N/A			$R\bar{3}$ (148)
$BiCl_3$	Group 15	103	N/A			*Cmcm* (63)
$ScCl_3$	Group 3	74.5	38235	$R\bar{3}$ (148)	Trigonal	
$LuCl_3$		86.1	N/A			$R\bar{3}$ (148)
YCl_3		90	15684	*C*2/*m* (12)	Monoclinic	
$YbCl_3$	Lanthanide	86.8	N/A			$R\bar{3}$ (148)
$TmCl_3$		88	35398	$R\bar{3}c$ (167)	Trigonal	
$ErCl_3$		89	N/A			*Cmcm* (63)
$HoCl_3$		90.1	N/A			*Cmcm* (63)
$DyCl_3$		91.2	40064	*Cmcm* (63)	Orthorhombic	
$TbCl_3$		92.3	40553	*Cmcm* (63)	Orthorhombic	
$GdCl_3$		93.5	22270	$P6_3/m$ (176)	Hexagonal	
$SmCl_3$		95.8	N/A			P63/m (176)
$NdCl_3$		98.3	31577	$P6_3/m$ (176)	Hexagonal	
$LaCl_3$		103.2	22267	$P6_3/m$ (176)	Hexagonal	
$AlBr_3$	Group 13	53.5	39768	$P2_1/c$ (14)	Monoclinic	
$GaBr_3$		62	413456	$P2_1/c$ (14)	Monoclinic	
$InBr_3$		80	65198	*C*2/*m* (12)	Monoclinic	
$TlBr_3$		88.5	N/A			$R\bar{3}$ (148)
$BiBr_3$	Group 15	103	100294	*C*2/*m* (12)	Monoclinic	
$ScBr_3$	Group 3	74.5	N/A			$R\bar{3}$ (148)
$LuBr_3$		86.1	N/A			*Cmcm* (63)
YBr_3		90	N/A			*Cmcm* (63)
$YbBr_3$	Lanthanide	86.8	56430	$R\bar{3}$ (148)	Trigonal	

$TmCl_3$		88	N/A			$R\bar{3}$ (148)
$ErBr_3$		89	N/A			$R\bar{3}$ (148)
$HoBr_3$		90.1	N/A			*Cmcm* (63)
$DyBr_3$		91.2	N/A			*Cmcm* (63)
$TbBr_3$		92.3	N/A			*Cmcm* (63)
$GdBr_3$		93.5	2610	*C*2/*m* (12)	Monoclinic	
$SmBr_3$		95.8	31591	*Cmcm* (63)	Orthorhombic	
$NdBr_3$		98.3	31590	*Cmcm* (63)	Orthorhombic	
$LaBr_3$		103.2	31581	$P6_3/m$ (176)	Hexagonal	
AlI_3	Group 13	53.5	391247	$P2_1/c$ (14)	Monoclinic	
GaI_3		62	413457	$P2_1/c$ (14)	Monoclinic	
InI_3		80	23136	$P2_1/c$ (14)	Monoclinic	
TlI_3		88.5	61349	*Pnma* (62)	Orthormbic	
BiI_3	Group 15	103	26083	$R\bar{3}$ (148)	Trigonal	
ScI_3	Group 3	74.5	N/A			$R\bar{3}$ (148)
LuI_3		86.1	N/A			$R\bar{3}$ (148)
YI_3		90	N/A			$R\bar{3}$ (148)
YbI_3	Lanthanide	86.8	N/A			$R\bar{3}$ (148)
TmI_3		88	N/A			$R\bar{3}$ (148)
ErI_3		89	N/A			$R\bar{3}$ (148)
HoI_3		90.1	N/A			$R\bar{3}$ (148)
DyI_3		91.2	N/A			$R\bar{3}$ (148)
TbI_3		92.3	N/A			$R\bar{3}$ (148)
GdI_3		93.5	N/A			*Cmcm* (63)
SmI_3		95.8	N/A			*Cmcm* (63)
NdI_3		98.3	N/A			*Cmcm* (63)
LaI_3		103.2	31596	*Cmcm* (63)	Orthormbic	

Table S4. Energy difference of MX_3 compared to the lowest energy structure among the six experimental structures. For example, $InCl_3$ exhibits the lowest total energy for the $R\bar{3}$ structure among the six experimental structures, and the values show the total energy difference compared to the energy of $R\bar{3}$ structure.

MX_3	$E_{tot} - E_{tot,\ lowest\ E}$ (meV/atom)						Most stale phase
	*C*2/*m* (12)	$P2_1/c$ (14)	*Cmcm* (63)	$R\bar{3}$ (148)	$R\bar{3}c$ (167)	$P6_3/m$ (176)	
$InCl_3$	1	94	111	0	61	133	$R\bar{3}$
$TlCl_3$	1	56	74	0	41	94	$R\bar{3}$
$BiCl_3$	26	55	0	26	27	16	*Cmcm*
$LuCl_3$	1	51	16	0	20	47	$R\bar{3}$
$YbCl_3$	1	28	4	0	18	32	$R\bar{3}$
$ErCl_3$	18	63	0	18	29	19	*Cmcm*
$HoCl_3$	30	51	0	29	38	14	*Cmcm*
$SmCl_3$	103	113	13	103	95	0	$P6_3/m$
$TlBr_3$	2	41	83	0	50	100	$R\bar{3}$
$ScBr_3$	2	66	74	0	73	99	$R\bar{3}$
$LuBr_3$	3	44	0	1	41	102	*Cmcm*
YBr_3	7	46	0	6	43	32	*Cmcm*
$TmBr_3$	2	46	21	0	46	54	$R\bar{3}$
$ErBr_3$	2	44	10	0	43	44	$R\bar{3}$
$HoBr_3$	3	44	0	1	41	34	*Cmcm*
$DyBr_3$	14	52	0	12	49	31	*Cmcm*
$TbBr_3$	25	61	0	23	57	27	*Cmcm*
ScI_3	4	72	79	0	79	106	$R\bar{3}$
LuI_3	3	61	66	0	70	87	$R\bar{3}$
YI_3	4	54	18	0	61	55	$R\bar{3}$
YbI_3	3	60	56	0	68	81	$R\bar{3}$
TmI_3	3	58	45	0	66	74	$R\bar{3}$
ErI_3	3	56	35	0	64	68	$R\bar{3}$
HoI_3	4	55	25	0	63	60	$R\bar{3}$
DyI_3	4	53	14	0	61	52	$R\bar{3}$
TbI_3	4	51	2	0	59	44	$R\bar{3}$
GdI_3	13	58	0	9	66	43	*Cmcm*
SmI_3	37	79	0	34	85	40	*Cmcm*
NdI_3	63	100	0	59	104	30	*Cmcm*

Table S5. Phase stability (decomposition energy, E_d) of Na_3MX_6 (X = Cl, Br, I) with the crystal structures of $P\bar{3}1c$, $P2_1/n$, $R\bar{3}$, $C2/m$ and $P\bar{3}m1$, against competing phases NaX and MX_3.

Na_3MX_6	Type of M	E_d (meV/atom)					Most stable phase	Stability
		$P\bar{3}1c$	$P2_1/n$	$R\bar{3}$	$C2/m$	$P\bar{3}m1$		
Na_3AlCl_6	Group 13	6.3	6.3	18.4	34.3	49.3	$P\bar{3}1c$	Metastable
Na_3GaCl_6		2.9	5.3	16.1	27.2	45.5	$P\bar{3}1c$	Metastable
Na_3InCl_6		-4.3	-2.0	1.8	14.0	24.7	$P\bar{3}1c$	Stable
Na_3TlCl_6		-1.7	2.3	2.6	12.0	23.8	$P\bar{3}1c$	Stable
Na_3BiCl_6	Group 15	-17.9	-20.8	-27.0	-12.8	-10.2	$R\bar{3}$	Stable
Na_3ScCl_6	Group 3	-3.5	-6.4	-0.5	16.0	22.7	$P2_1/n$	Stable
Na_3LuCl_6		-5.8	-10.3	-8.9	9.9	10.3	$P2_1/n$	Stable
Na_3YCl_6		-3.2	-9.2	-11.0	9.1	5.9	$R\bar{3}$	Stable
Na_3YbCl_6	Lanthanide	-5.2	-10.0	-9.1	9.8	9.5	$P2_1/n$	Stable
Na_3TmCl_6		-10.3	-15.7	-15.4	4.5	2.8	$P2_1/n$	Stable
Na_3ErCl_6		2.6	-2.8	-3.2	16.3	14.6	$R\bar{3}$	Stable
Na_3HoCl_6		7.9	2.2	1.2	20.9	18.5	$R\bar{3}$	Metastable
Na_3DyCl_6		13.2	7.1	5.4	25.4	22.3	$R\bar{3}$	Metastable
Na_3TbCl_6		18.6	12.1	9.5	30.0	26.0	$R\bar{3}$	Metastable
Na_3GdCl_6		25.1	18.0	14.7	35.5	30.7	$R\bar{3}$	Metastable
Na_3SmCl_6		42.8	34.5	28.9	50.9	43.8	$R\bar{3}$	Unstable
Na_3NdCl_6		61.2	50.8	42.7	66.2	56.6	$R\bar{3}$	Unstable
Na_3LaCl_6		76.1	63.3	52.4	78.0	64.8	$R\bar{3}$	Unstable
Na_3AlBr_6	Group 13	8.3	11.6	22.4	23.8	43.5	$P\bar{3}1c$	Metastable
Na_3GaBr_6		37.6	43.4	52.6	50.1	72.9	$P\bar{3}1c$	Unstable
Na_3InBr_6		10.6	17.1	20.6	18.5	37.0	$P\bar{3}1c$	Metastable
Na_3TlBr_6		11.2	19.7	20.4	17.1	36.0	$P\bar{3}1c$	Metastable
Na_3BiBr_6	Group 15	8.3	12.2	8.4	7.0	20.6	$C2/m$	Metastable
Na_3ScBr_6	Group 3	12.8	13.0	19.2	22.9	34.9	$P\bar{3}1c$	Metastable
Na_3LuBr_6		19.1	18.6	21.1	26.0	34.7	$P2_1/n$	Metastable
Na_3YBr_6		8.5	8.3	8.0	13.7	19.8	$R\bar{3}$	Metastable
Na_3YbBr_6	Lanthanide	6.3	6.2	8.3	13.1	21.5	$P2_1/n$	Metastable
Na_3TmBr_6		6.3	5.9	7.6	12.5	20.4	$P2_1/n$	Metastable

Na_3ErBr_6		6.2	5.9	7.1	12.3	19.9	$P2_1/n$	Metastable
Na_3HoBr_6		7.5	6.2	6.9	12.3	19.0	$P2_1/n$	Metastable
Na_3DyBr_6		11.1	11.0	10.6	16.1	22.4	$R\bar{3}$	Metastable
Na_3TbBr_6		16.1	15.3	14.4	20.0	25.9	$R\bar{3}$	Metastable
Na_3GdBr_6		6.2	6.1	3.8	9.8	15.1	$R\bar{3}$	Metastable
Na_3SmBr_6		32.4	30.4	27.0	33.6	37.6	$R\bar{3}$	Unstable
Na_3NdBr_6		43.8	41.0	35.7	43.6	45.5	$R\bar{3}$	Unstable
Na_3LaBr_6		58.4	54.1	46.4	56.6	55.2	$R\bar{3}$	Unstable
Na_3AlI_6	Group 13	42.2	47.3	54.0	46.4	64.8	$P\bar{3}1c$	Unstable
Na_3GaI_6		72.5	79.5	85.6	75.9	96.4	$P\bar{3}1c$	Unstable
Na_3InI_6		12.9	23.3	24.6	13.1	32.9	$P\bar{3}1c$	Metastable
Na_3TlI_6		79.1	91.2	90.1	78.1	98.5	$C2/m$	Unstable
Na_3BiI_6	Group 15	21.2	30.9	27.8	13.7	33.2	$C2/m$	Metastable
Na_3ScI_6	Group 3	28.0	30.6	35.3	30.1	42.7	$P\bar{3}1c$	Unstable
Na_3LuI_6		20.4	24.1	25.1	19.4	31.4	$C2/m$	Metastable
Na_3YI_6		17.6	22.7	21.8	16.2	27.3	$C2/m$	Metastable
Na_3YbI_6	Lanthanide	19.1	23.8	24.4	18.7	30.7	$C2/m$	Metastable
Na_3TmI_6		18.7	23.5	23.6	18.0	29.7	$C2/m$	Metastable
Na_3ErI_6		18.6	23.2	23.1	17.5	29.1	$C2/m$	Metastable
Na_3HoI_6		18.1	23.0	22.5	16.9	28.3	$C2/m$	Metastable
Na_3DyI_6		17.6	22.7	21.8	16.3	27.4	$C2/m$	Metastable
Na_3TbI_6		17.4	22.4	21.2	15.6	26.5	$C2/m$	Metastable
Na_3GdI_6		21.0	25.9	24.4	18.6	29.4	$C2/m$	Metastable
Na_3SmI_6		31.8	35.4	32.6	26.9	36.9	$C2/m$	Unstable
Na_3NdI_6		40.5	45.1	40.9	35.4	44.7	$C2/m$	Unstable
Na_3LaI_6		53.6	52.2	45.9	41.9	49.1	$C2/m$	Unstable

Table S6. Most stable structures of Na_3MX_6 (X = Cl, Br, I) among the crystal structures of $P\bar{3}1c$, $P2_1/n$, $R\bar{3}$, $C2/m$ and $P\bar{3}m1$, their decomposition energy, E_d, and stability against competing phases NaX and MX_3.

Type of M	M	M_{Radii} (pm)	Na_3MCl_6			Na_3MBr_6			Na_3MI_6		
			Most stable phase	E_d (meV/ atom)	Stability	Most stable phase	E_d (meV/ atom)	Stability	Most stable phase	E_d (meV/ atom)	Stability
Group 13	Al	54	$P\bar{3}1c$	6	Metastable	$P\bar{3}1c$	8	Metastable	$P\bar{3}1c$	42	Unstable
	Ga	62	$P\bar{3}1c$	3	Metastable	$P\bar{3}1c$	38	Unstable	$P\bar{3}1c$	72	Unstable
	In	80	$P\bar{3}1c$	-4	Stable	$P\bar{3}1c$	11	Metastable	$P\bar{3}1c$	13	Metastable
	Tl	89	$P\bar{3}1c$	-2	Stable	$P\bar{3}1c$	11	Metastable	$C2/m$	78	Unstable
Group 15	Bi	103	$R\bar{3}$	-27	Stable	$C2/m$	7	Metastable	$C2/m$	14	Metastable
Group 3	Sc	75	$P2_1/n$	-6	Stable	$P\bar{3}1c$	13	Metastable	$P\bar{3}1c$	28	Unstable
	Lu	86	$P2_1/n$	-10	Stable	$P2_1/n$	19	Metastable	$C2/m$	19	Metastable
	Y	90	$R\bar{3}$	-11	Stable	$R\bar{3}$	8	Metastable	$C2/m$	16	Metastable
Lanthanide	Yb	87	$P2_1/n$	-10	Stable	$P2_1/n$	6	Metastable	$C2/m$	19	Metastable
	Tm	88	$P2_1/n$	-16	Stable	$P2_1/n$	6	Metastable	$C2/m$	18	Metastable
	Er	89	$R\bar{3}$	-3	Stable	$P2_1/n$	6	Metastable	$C2/m$	17	Metastable
	Ho	90	$R\bar{3}$	1	Metastable	$P2_1/n$	6	Metastable	$C2/m$	17	Metastable
	Dy	91	$R\bar{3}$	5	Metastable	$R\bar{3}$	11	Metastable	$C2/m$	16	Metastable
	Tb	92	$R\bar{3}$	9	Metastable	$R\bar{3}$	14	Metastable	$C2/m$	16	Metastable
	Gd	94	$R\bar{3}$	15	Metastable	$R\bar{3}$	4	Metastable	$C2/m$	19	Metastable
	Sm	96	$R\bar{3}$	29	Unstable	$R\bar{3}$	27	Unstable	$C2/m$	27	Unstable
	Nd	98	$R\bar{3}$	43	Unstable	$R\bar{3}$	36	Unstable	$C2/m$	35	Unstable
	La	103	$R\bar{3}$	52	Unstable	$R\bar{3}$	46	Unstable	$C2/m$	42	Unstable

Table S7. Phase stability (decomposition energy, E_d) of Na_3MX_6 (X = Cl, Br, I) against the competing phases $NaMX_4$ (space group: $P2_12_12_1$) and NaX for the relatively small M with the ionic radii below 80 pm.

	M	X	r_M (pm)	r_X (pm)	Octahedral factor MX_6 (r_M / r_X)	Decomposition energy (meV/atom)	Stability
Na_3AlCl_6	Al	Cl	54	181	0.30	21	Metastable
Na_3GaCl_6	Ga	Cl	62	181	0.34	41	Unstable
Na_3InCl_6	In	Cl	80	181	0.44	-26	Stable
Na_3ScCl_6	Sc	Cl	75	181	0.41	-35	Stable
Na_3AlBr_6	Al	Br	54	196	0.28	36	Unstable
Na_3GaBr_6	Ga	Br	62	196	0.32	58	Unstable
Na_3InBr_6	In	Br	80	196	0.41	-6	Stable
Na_3ScBr_6	Sc	Br	75	196	0.38	-27	Stable
Na_3AlI_6	Al	I	54	220	0.25	55	Unstable
Na_3GaI_6	Ga	I	62	220	0.28	79	Unstable
Na_3InI_6	In	I	80	220	0.36	19	Metastable
Na_3ScI_6	Sc	I	75	220	0.34	-45	Stable

Table S8. Na-ion migration energy barrier (E_a) in Na_3MX_6 (M = In, Er, Gd; X = Cl, Br) and Na_3GdI_6, predicted using the BVSE method.

	Crystal system	Space group	E_a (eV)	
			1D	3D
Na_3InCl_6	Trigonal	$P\bar{3}1c$	0.45	0.53
Na_3ErCl_6	Monoclinic	$P2_1/n$	N/A	0.60, 0.70
Na_3GdCl_6	Trigonal	$R\bar{3}$	0.35	0.65
Na_3InBr_6	Trigonal	$P\bar{3}1c$	0.42	0.49
Na_3ErBr_6	Monoclinic	$P2_1/n$	N/A	0.52, 0.54
Na_3GdBr_6	Trigonal	$R\bar{3}$	0.31	0.52
Na_3GdI_6	Monoclinic	$C2/m$	N/A	0.48

Table S9. Predicted Na-ion conductivity at 300 K and the activation energy of Na_3InBr_6, Na_3GdBr_6, Na_3YI_6 and Na_3GdI_6 from the Arrhenius plots of Na-ion conductivity.

	Activation energy, E_a (eV)	Ionic conductivity (S cm^{-1})	Ionic conductivity Error bound [min, max] (S cm^{-1})
Na_3YI_6 (*C2/m*)	0.34 ± 0.02	2.4×10^{-4}	[8.6×10^{-5}, 6.9×10^{-4}]
Na_3GdI_6 (*C2/m*)	0.30 ± 0.01	5.9×10^{-4}	[3.5×10^{-4}, 1.0×10^{-3}]
Na_3InBr_6 ($P\bar{3}1c$)	0.37 ± 0.01	5.8×10^{-5}	[2.9×10^{-5}, 1.2×10^{-4}]
Na_3GdBr_6 ($R\bar{3}$)	0.50 ± 0.03	1.2×10^{-6}	[2.3×10^{-7}, 6.5×10^{-6}]

Table S10. Phase stability (decomposition energy, E_d) of $Na_3MBr_xI_{6-x}$ (M = Y, Gd) with the crystal structures of $R\bar{3}$ and $C2/m$.

$Na_3MBr_xI_{6-x}$	x	Composition	E_D (meV/atom)		Phase preference
			$C2/m$	$R\bar{3}$	
$Na_3YBr_xI_{6-x}$	0	Na_3YI_6	16	22	$C2/m$
	1	Na_3YBrI_5	17	22	$C2/m$
	2	$Na_3YBr_2I_4$	18	22	$C2/m$
	3	$Na_3YBr_3I_3$	19	20	$C2/m$
	4	$Na_3YBr_4I_2$	18	17	$R\bar{3}$
	5	Na_3YBr_5I	13	13	$R\bar{3}$
	6	Na_3YBr_6	14	8	$R\bar{3}$
$Na_3GdBr_xI_{6-x}$	0	Na_3GdI_6	19	24	$C2/m$
	1	Na_3GdBrI_5	19	24	$C2/m$
	2	$Na_3GdBr_2I_4$	18	23	$C2/m$
	3	$Na_3GdBr_3I_3$	17	20	$C2/m$
	4	$Na_3GdBr_4I_2$	14	16	$C2/m$
	5	Na_3GdBr_5I	10	11	$R\bar{3}$
	6	Na_3GdBr_6	10	4	$R\bar{3}$

Table S11. Predicted Na-ion conductivity at 300 K and the activation energy of $Na_3YBr_3I_3$ and $Na_3GdBr_3I_3$ from the Arrhenius plots.

	Activation energy, E_a (eV)	Ionic conductivity (S cm^{-1})	Ionic conductivity Error bound [min, max] (S cm^{-1})
$Na_3YBr_3I_3$ (*C2/m*)	0.25 ± 0.02	3.3×10^{-3}	[1.5×10^{-3}, 7.4×10^{-3}]
$Na_3GdBr_3I_3$ (*C2/m*)	0.21 ± 0.02	7.5×10^{-3}	[3.2×10^{-3}, 1.8×10^{-2}]

Table S12. Electrochemical stability window of Na_3MX_6 (X = Cl, Br, I) including phase equilibria at reduction and oxidation potentials.

Na_3MX_6	Type of M	Reduction Potential (V)	Phase equilibria at the reduction potential	Oxidation Potential (V)	Phase equilibria at the oxidation potential
Na_3InCl_6	Group 13, 15	2.14	InCl, NaCl	4.08	$NaCl_3$, $InCl_3$
Na_3BiCl_6		2.25	Bi, NaCl	3.94	$NaCl_3$, $BiCl_3$
Na_3ScCl_6	Group 3	0.85	Sc_5Cl_8, NaCl	3.76	$NaScCl_4$, $NaCl_3$
Na_3LuCl_6		0.56	Lu, NaCl	3.77	$NaCl_3$, $NaLuCl_4$
Na_3YCl_6		0.53	Y, NaCl	3.82	$NaCl_3$, YCl_3
Na_3TmCl_6	Lanthanide	0.55	Tm, NaCl	3.86	$NaCl_3$, $TmCl_3$
Na_3ErCl_6		0.52	Er, NaCl	3.86	$NaCl_3$, $NaErCl_4$
Na_3HoCl_6		0.52	Ho, NaCl	3.92	$NaCl_3$, $NaHoCl_4$
Na_3DyCl_6		0.52	Dy, NaCl	3.89	$NaCl_3$, $DyCl_3$
Na_3TbCl_6		0.52	Tb, NaCl	3.87	$NaCl_3$, $TbCl_3$
Na_3GdCl_6		0.53	Gd, NaCl	3.88	$NaGdCl_4$, $NaCl_3$
Na_3InBr_6	Group 13, 15	2.19	$InBr_2$, NaBr	3.70	$InBr_3$, Br
Na_3BiBr_6		2.14	Bi, NaBr	3.70	$BiBr_3$, Br
Na_3ScBr_6	Group 3	0.84	Sc, NaBr	3.80	$ScBr_3$, Br
Na_3LuBr_6		0.69	Lu, NaBr	3.76	$LuBr_3$, Br
Na_3YBr_6		0.62	Y_2Br_3, NaBr	3.70	YBr_3, Br
Na_3TmBr_6	Lanthanide	0.67	Tm, NaBr	3.75	$TmBr_3$, Br
Na_3ErBr_6		0.62	Er, NaBr	3.70	$ErBr_3$, Br
Na_3HoBr_6		0.67	Ho, NaBr	3.75	$HoBr_3$, Br
Na_3DyBr_6		0.62	Dy, NaBr	3.77	$DyBr_3$, Br
Na_3TbBr_6		0.62	Tb, NaBr	3.77	$TbBr_3$, Br
Na_3GdBr_6		0.61	Gd, NaBr	3.70	$GdBr_3$, Br
Na_3InI_6	Group 13, 15	1.93	InI, NaI	2.93	$NaInI_4$, I
Na_3BiI_6		1.91	Bi, NaI	2.93	BiI_3, I
Na_3ScI_6	Group 3	1.42	$Na(ScI_3)_2$, NaI	2.98	ScI_3, I
Na_3LuI_6		0.74	Lu, NaI	2.99	LuI_3, I
Na_3YI_6		0.63	Y, NaI	2.93	YI_3, I
Na_3TmI_6	Lanthanide	0.72	Tm, NaI	2.98	TmI_3, I
Na_3ErI_6		0.70	Er, NaI	2.99	ErI_3, I
Na_3HoI_6		0.69	Ho, NaI	2.97	HoI_3, I
Na_3DyI_6		0.69	Dy, NaI	2.97	DyI_3, I
Na_3TbI_6		0.68	Tb, NaI	2.97	TmI_3, I
Na_3GdI_6		0.65	Gd, NaI	2.96	GdI_3, I